Deamidation of Human γS-Crystallin Increases Attractive Protein Interactions: Implications for Cataract

Ajay Pande, **Natalya Mokhor**[†], and **Jayanti Pande**[*]
Department of Chemistry, Life Sciences 2070, University at Albany, State University of New York, Albany, New York 12222, United States

Abstract

Deamidation of proteins is one of the most prevalent post-translational modifications found upon aging, and in age-onset diseases. Specific asparagine and glutamine residues are often selectively deamidated during this process. In the human lens, deamidation has been shown to occur in many crystallins, but it is not clear how these deamidated proteins lead to lens opacity or cataract. Here we have modeled *in vitro* the effect of deamidation of specific asparagine and glutamine residues in human recombinant γS-crystallin (HGS) on the solution properties of the protein. The residues selected for deamidation *in vitro* are those that are found to be deamidated in aged and cataractous lenses *in vivo*. Two derivatives were prepared, one with Asn76 and Asn143 deamidated (2N-HGS) and the other with two additional Gln residues (92 and 120) deamidated (2N2Q-HGS). Isoelectric focusing measurements showed the expected lowering of the pI from 6.9 in HGS to ~6.5 in 2N-HGS and to ~6.1 in 2N2Q-HGS. However, spectroscopic studies showed no significant change in the secondary and tertiary structures of the deamidated proteins relative to the wild type. The stability of 2N-HGS and 2N2Q-HGS, as measured by guanidinium hydrochloride unfolding, also remained comparable to that of HGS. The main difference was the altered protein–protein interaction among the three proteins. The net repulsive interactions that are characteristic of HGS are diminished in the deamidated derivatives as evidenced by static light scattering measurements of the second virial coefficient, B_2 (B_2 values for HGS, 2N-HGS, and 2N2Q-HGS of 8.90×10^{-4}, 7.10×10^{-4}, and 6.65×10^{-4} mL mol g^{-2}, respectively). Further substantiation is provided by estimates of the excess binding energy of protein–protein interactions in the condensed phase, obtained from measurements of the PEG-induced liquid–liquid phase separation profiles for the three proteins. The data suggest that enhanced attractive protein–protein interactions, arising from the deamidation of HGS, promote protein aggregation, thereby leading to increased light scattering and opacity over time.

Graphical abstract

[*]**Corresponding Author:** Department of Chemistry, Life Sciences 2076, University at Albany, State University of New York, 1400 Washington Ave., Albany, NY 12222. jpande@albany.edu. Telephone: 518-591-8842.
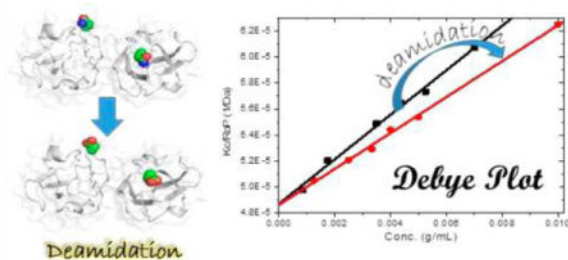[†]**Present Address:** N.M.: Pennsylvania College of Optometry, Salus University, 8360 Old York Rd., Elkins Park, PA 19027.

Notes
The authors declare no competing financial interest.

Nonenzymatic deamidation of neutral amino acid residues asparagine and glutamine to the acidic aspartic and glutamic residues, respectively, often occurs spontaneously upon aging *in vivo*.[1–3] Such deamidation is also observed *in vitro* upon the aging of proteinaceous material, for example, woolen textiles,[4] works of art,[5] and foodstuffs.[6] However, not all Asn and Gln residues are deamidated equally readily. The rate of deamidation varies considerably and depends on the location of the residues in the primary,[7] secondary,[8,9] and tertiary structures[10] of the proteins, the surface exposure,[11] and their surrounding environment.[12,13]

Proteins in the human ocular lens are probably the most extensively studied entities with regard to deamidation. Age-related deamidation is observed not only in the lens crystallins, the predominant proteins in the lens, but also in other lens proteins.[14–16] Because the concentration of crystallins is at least 2 orders of magnitude higher than that of other lens proteins, and the rate of protein turnover is low in lens fiber cells, there is substantial accumulation of the products of post-translational modifications (PTMs) of the crystallins, such as deamidation, over time.[16] This may result in aging-related deterioration of the lens, increasing its opacity and leading to cataract.

Deamidation of crystallins with aging was noted long ago,[17,18] and in recent years, the effects of many such amide to acid substitutions in crystallins have been studied *in vitro*. Chaves et al.[19] separately examined the effects of deamidation of both Asn101 and Asn123 on the structure and chaperone function of human αA-crystallin and found that there were changes in secondary and tertiary structure in both cases. The chaperone activity was also lowered, but the effect was more pronounced in the Asn123-deamidated product. Similarly, in human αB-crystallin, the effect of deamidation on the structure and chaperone activity was larger in the case of Asn146 than in the case of Asn78.[20] The most extensive study of the effect of deamidation has probably been conducted on the β-crystallins.[16] In βA3-crystallin, deamidations of Asn133 and Asn155 in the C-terminal domain and Asn120 in the domain-connecting peptide have a stronger effect on disrupting protein tertiary structure than the deamidation of Gln42 and Asn54 in the N-terminal domain.[21] Thus, as in the case of α-crystallin, the effect of deamidation in β-crystallin also shows that the severity due to this protein modification depends on the spatial location of the deamidated residue in the protein structure. In contrast, deamidation of Gln70 and Gln162 in βB2-crystallin leads to a destabilization of the native dimer,[22] even though the overall structural changes are minimal. Notably, however, the doubly deamidated derivative of βB2-crystallin shows a greater degree of structural change relative to the individual, singly deamidated products, which suggests that the structural changes due to deamidation are synergistic in this case.

To the best of our knowledge, such extensive studies of deamidations that serve as mimics of aging and cataract have not been reported for the γ-crystallins. Flaugh et al.[23] have examined the effect of deamidation of Gln54 and Gln143 on the structure and stability of human γD-crystallin (HGD), but as acknowledged by the authors, the selection of these Gln residues for deamidation was based on structural considerations rather than on their reported presence in aged or cataractous lenses. Nonetheless, in the case of human γS-crystallin (HGS), there is ample evidence of the deamidation of specific Asn and Gln residues *in vivo*.[1,11,24–31] Therefore, for the *in vitro* studies presented here, we selected residues in HGS for deamidation based on the weight of the currently available evidence of their presence in aged and cataractous lenses. We report on studies of two deamidated derivatives of HGS produced recombinantly: the first in which Asn76 and Asn143 have been substituted with the corresponding Asp residues (named 2N-HGS) and a second, more extensively deamidated derivative in which two Gln residues (92 and 120) were substituted with Glu (named 2N2Q-HGS), in addition to the already substituted Asn residues. Deamidation of Asn76 in HGS has been shown to be associated with human cataract by Hooi et al.,[26] and deamidated Asn143 has been observed in the high-molecular weight fraction from human lens homogenate,[11,27] which is a proxy for age-onset changes. Evidence for the age-associated deamidation of Gln92 in HGS comes from several studies, namely those of Hanson et al.,[30] Hains et al.,[31] and Hooi et al.,[26] and the deamidation of Gln120 has been shown by Wilmarth et al.[29] and Hains et al.[31]

As stated above, several Asn and Gln residues in HGS are known to be deamidated upon aging and in cataract; thus, the selection of residues to mimic the effect of deamidation *in vitro* was difficult. It was already known that the deamidation of a single residue in βB2[22] and βA3[32] crystallins leads to minimal structural change, and this effect is often synergistic (additive) when multiple residues are deamidated and becomes substantive (discussed above). Therefore, for the first mimic, we selected two Asn residues as models of deamidation at lower levels (2N-HGS), and for the more extensive deamidation mimic, we selected two additional Gln residues (2N2Q-HGS). We concluded that these two test samples would serve as reasonable mimics of deamidated HGS *in vivo* and also inform on the role of Asn and Gln deamidation.

We are aware that deamidation is often followed by racemization, isomerization, and even truncation,[16] which are at present rather difficult to model *in vitro*. By selecting this particular set of residues and simply substituting amide groups with the corresponding acid residues, we expected at the very least (i) to probe the effect of negative charges in specific locations, (ii) to observe relative differences between Asn and Gln modifications, and (iii) to determine the effect of an overall increase in negative charge on the structure and solution properties of HGS. The results provide mechanistic clues that suggest how these PTM mimics could promote lens opacity.

EXPERIMENTAL PROCEDURES

Protein Expression and Purification

Human γS-crystallin cDNA cloned in the pET3a vector was a generous gift from N. Lubsen (Radboud University, Nijmegen, The Netherlands). HGS and the two mutants with specific

residues deamidated, were expressed in *Escherichia coli*: 2N-HGS has Asn76 and Asn143 replaced with Asp, which models a product with a lower level of deamidation, and 2N2Q-HGS has replacements of Gln92 and Gln120 with Glu, in addition to changes of Asn76 and Asn143 to Asp, and models an extensively deamidated product. The locations of these residues in the structure of HGS are shown in Figure 1.

Mutations were introduced using the Quickmut site-directed mutagenesis kit from Agilent, with the following forward primers and their reverse complements: Asn76, 5′-GGA TGG GCC TCG ACG ACC GCC TCA GC-3′; Asn143, 5′-GAG CTA CCC GAC TAC CGT GGC AGG C-3′; Gln92, 5′-CTG CCC AGT GGA GGC GAG TAT AAG ATT CAG-3′; Gln120, 5′-GCC TCC CCA GCT GTC GAG TCT TTC CGC CGC ATT GTG GAG-3′. cDNA was isolated from *E. coli* cells containing the WT and mutant nucleotide sequences using the classical ZR Plasmid Miniprep kit (Zymo Research) and sequenced by Eurofins MWG Operon. At first, four constructs, each with a single mutation of residue 76, 143, 92, or 120, were made. After sequencing data showed the correct expected sequence, multiple mutated constructs were made, one step at a time, and at each successive step, cDNA was sequenced and confirmed. For protein expression, only two constructs were used, one with Asn76 and Asn143 mutated, and the other with the additional residues Gln92 and Gln120 mutated.

Protein expression and purification procedures were similar to those used for human γD-crystallin[33] and are summarized here. HGS and mutants were expressed in *E. coli* BL21(DE3) cells grown at 37 °C to an absorbance of ~0.7. Isopropyl β-D-1-thiogalactopyranoside (IPTG) at a final concentration of 1 mM was used to induce overexpression of the protein. Cell lysis was conducted in 5 mM Tris-HCl buffer (pH 8) containing 25 mM NaCl, 2 mM EDTA, protease inhibitor (1 tablet of Complete/ 25 mL of lysis buffer, Roche biochemical), and lysozyme (250 μg/mL), with five rapid freeze–thaw cycles alternating between freezing in liquid nitrogen and thawing in water at 30 °C. The lysate was centrifuged at 48000*g* following incubation with 25 μg/mL DNase (Sigma). The supernatant containing >90% of the protein was collected. Pure HGS and the mutants were isolated from the supernatant by size-exclusion chromatography, followed by cation-exchange chromatography.[33] Protein purity was assessed by SDS–PAGE for all three proteins and by electrospray ionization mass spectrometry (ESIMS) analysis for HGS at the Center for Functional Genomics at the University at Albany. The mass spectrometry results gave an average mass of 20875 ± 1 Da for HGS. The "theoretical" value of the mass computed from the protein sequence (www.expasy.ch) is 20875, which is in excellent agreement with the mass spectrometry result. The deamidated mutants were not subjected to routine ESIMS analysis because of the difficulty of detecting mass changes of ±1 following deamidation. These were characterized instead by isoelectric focusing (IEF) as described below. Because cDNA sequencing and IEF data confirmed that the correct deamidation products were produced, no further analysis was conducted on the deamidated derivatives to confirm the substitutions.

Gel Electrophoresis

SDS–PAGE analyses were performed on a Bio-Rad Mini-Protean-II gel electrophoresis system, using 12% polyacrylamide gels under reducing and nonreducing conditions, according to the protocols provided in the Bio-Rad manuals. IEF runs were made on a model 111 mini IEF apparatus from Bio-Rad. Coomassie Blue R-250 dye and crocein scarlet were used to detect the protein bands.

Circular Dichroism and Tryptophan Fluorescence

Comparisons of the secondary and tertiary structures of the three proteins were made by measurements of the CD and tryptophan fluorescence emission spectra. CD measurements were taken on a Jasco J-815 spectropolarimeter. Near-UV CD spectra were measured at protein concentrations of 1 mg/mL in 0.1 M sodium phosphate buffer (pH 7) using a 10 mm path length. For the far-UV CD spectra, protein concentrations of 0.1 mg/mL were used in a 1 mm path length cuvette and normalized with respect to the peptide backbone concentration.

Tryptophan fluorescence spectra were measured with a Horiba Jobin Yvon Fluorolog-3 spectrofluorometer at a protein concentration close to that used for the far-UV CD measurements (0.1 mg/mL), in 0.1 M sodium phosphate buffer (pH 7). The excitation wavelength was set at 290 nm, and both slits were set at 5 nm.

Chemical Stability Measurements

Guanidinium hydrochloride (GdnHCl)-mediated unfolding monitored by tryptophan fluorescence emission was used to determine the relative chemical stabilities of the three proteins. Samples at protein concentrations of 0.1 mg/mL were incubated with increasing concentrations of GdnHCl [0–5 M in 0.1 M sodium phosphate buffer (pH 7)] at 25 °C for approximately 5–6 h before measurement. The ratios of fluorescence intensities at 360 and 320 nm ($I_{360/320}$) were plotted as a function of GdnHCl concentration, and the midpoints of the transitions were estimated using first-derivative spectra for each protein.

Assessment of Protein–Protein Interactions

The strengths of protein–protein interactions in solution were estimated (i) by measuring the second virial coefficient, B_2, using static light scattering and (ii) by performing polyethylene glycol (PEG)-induced liquid–liquid phase separation (LLPS). Static light scattering studies for part (i) were conducted at 25 °C using the Malvern Zetasizer Nano-S to determine B_2 using toluene as the standard scattering reference. The refractive index increment, dn/dc, value of 0.193[34] was used for all three proteins. This represents the peak of a wide distribution of values for the crystallins, in which the γ-crystallins generally represent the higher end at ~0.199.[35] However, these values are often derived from measurements at wavelengths lower than 633 nm (which was used for our light scattering measurements). Therefore, we chose the more conservative value. Debye plots were made according to eq 1 from which B_2 and molecular weights were calculated using the manufacturer-supplied DTS software. The measured molecular weights also provided a check on the accuracy of the results. Where appropriate, the observed scattering intensity was corrected as suggested by Yadav et al.[36]

$$\frac{KC}{R_\theta} = \frac{1}{M_W} + 2B_2 C \tag{1}$$

where K is the optical constant given by $K = [2\pi^2 n^2 (dn/dc)^2]/(\lambda_0^4 N_A)$, R_θ the excess Rayleigh ratio, M_W the weight-average molecular weight of the protein, C the protein concentration in grams per milliliter, λ_0 the wavelength of incident light, B_2 the second virial coefficient, (dn/dc) the refractive index increment, and N_A Avogadro's number.

PEG-induced liquid–liquid phase separation experiments for part (ii) were performed according to the method of Wang et al.[37] Stock solutions of PEG 8000 (Sigma Ultra) and protein solutions (12.5 mg/mL) were prepared in 0.1 M phosphate buffer (pH 7) containing 0.01% sodium azide. Equal volumes of PEG and protein solutions were mixed at 4 °C in the cold room to induce phase separation. These conditions were first determined in a pilot experiment to be appropriate for inducing phase separation. After 24 h at 4 °C, the protein concentration in the dilute phase was measured for various solutions with different PEG concentrations as shown in Figure 6A. From these data, the chemical potential of proteins in the dense phase was determined,[37] which provided E_B, the excess binding energy in the mutant proteins relative to the wild-type (Figure 6B and Table 1), in the following manner, starting with eq 2.[37]

$$\ln\left(\frac{\nu_0 N_A}{M_1} c_1^I\right) = -\frac{\varepsilon_B}{kT} - \Delta\nu\frac{\Pi_2}{kT} \tag{2}$$

where c_1^I is the solubility (i.e., protein mass concentration in the supernatant dilute phase), M_1 the molecular weight of the protein, N_A Avogadro's number, k Boltzmann's constant, T the absolute temperature, ν_0 the volume per protein molecule in the condensed phase, ν the difference in the excluded volume of PEG per protein molecule in the dilute and condensed phases, and ε_B the molecular binding energy.

Subtracting $\ln[(\nu_0 N_A)/(M_1)c_0]$, where c_0 is the starting protein concentration, from both sides and rearranging gives

$$\ln\left(\frac{c_1^I}{c_0}\right) = -\underbrace{\left[\ln\left\{\frac{\nu_0 N_A}{M_1}c_0\right\} + \frac{E_B}{RT}\right]}_{\text{(free energy term)}} - N_A\Delta\nu\left(\frac{\Pi_2}{N_A kT}\right) \tag{3}$$

We plot the expression on the left as a function of the expression on the right as shown in Figure 6B.

In the expression for the free energy (first term on the right) in eq 3, ν_0 and E_B are the only two unknown quantities. The former is a constant for similarly shaped molecules (such as HGS and the mutants). Thus, the intercept of the resulting linear plot will give us the free energy of formation of the condensed phase for all three proteins. However, because ν_0 is

not known, we can obtain only the difference in free energy for the mutants relative to HGS (i.e., ΔE_B, see Table 1). The slope of the line provides $N_A \Delta \nu$, the difference in the PEG-excluded volume per mole of protein in the dilute and condensed phases. Thus, by inducing phase separation using PEG, we can calculate the change in the binding energy of deamidated HGS, which is an intrinsic property of these proteins and is independent of PEG.

RESULTS AND DISCUSSION

Figure 2A shows the IEF analysis of HGS and the two mutants and reveals the expected downshift of the isoelectric point (pI) upon deamidation. The pI values of the two mutants become progressively more acidic as the protein gains additional negative charges. Thus, the shift in pI upon the deamidation of two Asn residues is ~0.4 pH unit on average (pI $\cong$ 6.5 for 2N-HGS relative to HGS with a pI $\cong$ 6.9), and the additional deamidation of two Gln residues in 2N2Q-HGS lowers the pI further by ~0.4 pH unit on average (pI ≈ 6.1 for 2N2Q-HGS). These small differences in pI values were reproducible across several IEF runs. The computed pI values for HGS, 2N-HGS, and 2N2Q-HGS are 6.42, 5.84, and 5.45, respectively (www.expasy.ch), all shifted lower by ~0.6 pH unit, and are reasonably close to the experimentally measured values. We noticed mainly two bands for each protein in the IEF gels, which reduce to predominantly a single band when the samples are treated with excess DTT. This suggests that intramolecular disulfide linkages are present in all three proteins prior to reduction.

The corresponding SDS–PAGE analysis is presented in Figure 2B for all three proteins, again with and without reduction with excess DTT. Here we found that the reduced protein samples consistently appear to be slightly larger in size (~1 kDa) than the nonreduced samples. The small, apparent increase in size may arise from somewhat loosely structured, extended forms of the protein molecules in the reduced state, because intramolecular disulfide linkages that would typically impose structural constraints are absent.

Figure 3 shows that the lowering of pI in the mutants does not appreciably alter their secondary and tertiary structures, and all three proteins remain fully folded. In Figure 3A, we compare the far-UV CD spectra of the wild-type and deamidated proteins and find them to be nearly identical, and typical of predominantly β-sheet-containing proteins with a trough around 217 nm and a peak around 190 nm. The near-UV CD region (Figure 3B), while also closely similar for all three proteins, shows small differences in the regions attributed to aromatic residues, especially tryptophan (280–320 nm).[38] Because the only Trp residue that is close to Asp76 is Trp72, ~3 Å distant (Figure 1), the deamidation of Asp76 could affect the environment of Trp72 in both mutants. The change in protein sequence upon deamidation from ^{76}ND^{78}R to ^{76}DD^{78}R is likely to affect the hydrogen bonding pattern in the region surrounding Trp72, possibly leading to the minor changes observed in the Trp region of the near-UV CD spectrum (Figure S1 of the Supporting Information).

These subtle changes in the environment of Trp72 are also evident in the small differences in the tryptophan fluorescence intensities shown in Figure 3C. Deamidation of Asn76 and Asn143 in 2N-HGS leads to a slight broadening of the emission spectrum and a small increase in the Trp fluorescence intensity while leaving the λ_{max} essentially unchanged.

Interestingly, however, the additional deamidation of Gln residues 92 and 120 in 2N2Q-HGS results in a partial recovery of the fluorescence intensity while, again, maintaining the λ_{max} close to that of HGS. Such small variations in the quenching of Trp fluorescence by neighboring groups are not surprising because quenching is a distance-dependent phenomenon and minor adjustments in tertiary structure upon deamidation may be revealed in the fluorescence intensity.

In addition to changes in the Trp region, the near-UV CD spectra (Figure 3B) also show minor differences around 260–280 nm attributed to Phe and Tyr residues.[38] While it is difficult to make structural correlations with such changes, we note that N143 and Q92 in the primary structure of HGS are followed by a Tyr residue, and Q120 is followed by a Phe residue. Thus, it is conceivable that these aromatic residues act as reporters of deamidation-mediated changes in their H-bonding environment. We recognize that the observed changes are small and could simply arise from the reorganization of the side chains following deamidation, but given that (i) all the deamidations examined in this study occur at predominantly surface-exposed residues known to be involved in H-bonding and (ii) the γ-crystallins are characterized by a preponderance of salt bridges involving acidic and basic residues on the surface,[39] the emphasis on the involvement of the H-bonding network in the observed deamidation-mediated spectral changes seems reasonable.

We also examined the deamidated derivatives for changes in stability if any, relative to that of the wild type, using chemical unfolding with GdnHCl. This well-established method measures the structural stability of proteins,[40] by progressively unfolding the protein and monitoring the solvent exposure of buried Trp residues. Figure 4 shows the Trp fluorescence emission spectra as a function of the increasing concentration of GdnHCl and reveals only minor differences in the unfolding equilibrium of the deamidated versus wild-type proteins. The midpoint of the unfolding transition lies at ~2.6 ± 0.1 M GdnHCl for all three proteins ($C_{m,HGS}$ = 2.6 M, $C_{m,2N-HGS}$ = 2.7 M, and $C_{m,2N2Q–HGS}$ = 2.5 M, where C_m is the midpoint of the transition), as deduced from the first-derivative spectrum of each unfolding curve. This result is in contrast to the protein destabilization observed in HGD following the deamidation of two Gln residues.[23] It should be noted that the Gln residues in HGD[23] were interfacial residues residing between the two protein domains. In the case of the 2N2Q-HGS derivative, although the Gln92 is in the domain-connecting peptide, it is close to the C-terminus, and away from the domain interface region (Figure 1), as shown by the NMR structure of HGS.[41] Deamidation at critical structural regions has also been shown to decrease the stability of the β-crystallins.[21,32,42] Here the decrease in stability may be due to the disruption of inter- and intramolecular pairing of domains required to maintain the overall structural integrity of the protein. Thus, deamidation seems to interfere with a key structural feature[16] of the β-crystallins.

γS-Crystallin (GS) is known to have a unique place in the γ-crystallin family and was initially considered to be a member of the β-crystallin family (named β-$_{Slow}$ or βS-crystallin), based mainly on the chromatographic profile of bovine γS-crystallin (BGS).[43] This was later corrected by Bloemendal and colleagues, who noticed its greater similarities to the members of the γ-crystallin family.[44] Its solution properties are rather distinct from those of most other γ-crystallins, and it does not spontaneously undergo liquid–liquid phase

separation (at temperatures above −10 °C).[45] This behavior, distinct from that of the other γ-crystallins, is indicative of net repulsive protein–protein interactions among molecules of BGS. Net repulsive interactions may also explain why attempts to crystallize intact GS have thus far been unsuccessful. In mixtures with other γ-crystallins, BGS lowers the demixing (clouding) temperature[46] and also dramatically slows their aggregation mediated by the oxidation of protein sulfhydryl groups.[47] We suggested previously[47] that these properties of GS are potentially beneficial for maintaining transparency, or delaying opacity, in the lens.

In view of our observations that deamidated HGS mutants, even the extensively deamidated HGS mimic, maintain structures and stabilities comparable to those of the wild-type protein, it was especially important to assess whether these modifications had any effect on the nature and magnitude of the self (homologous), protein–protein interactions. We have already shown for several cataract-associated γ-crystallin mutants that changes in homologous (i.e., self) interactions result from a single-point mutation.[33,48,49] Therefore, to evaluate possible changes in self-interactions upon deamidation, we used two well-established probes: liquid–liquid phase separation (LLPS) and the second virial coefficient (B_2).

LLPS can be induced in GS by means of PEG.[45] Using PEG-induced LLPS as a tool, it is possible to qualitatively and comparatively estimate the attractive interactions in proteins, as well as to obtain quantitative thermodynamic parameters of these interactions,[37] as already described in Experimental Procedures. Another measure of the self-interaction among proteins in solution is the magnitude and sign of the second virial coefficient (B_2). Attractive interactions lead to lowering of the osmotic pressure from its "ideal solution" manifestation, and vice versa. Thus, a positive value of B_2 shows repulsive interactions: The greater the magnitude of B_2, the stronger the net repulsive interaction. Early work by Tardieu and co-workers showed that, in general, the β-crystallins are characterized by net repulsive interactions and the γ-crystallins by net attractive interactions under physiological solution conditions.[50]

Figure 5 shows our measurements of B_2 for HGS and the deamidated derivatives, using static light scattering. A positive B_2 value (8.9×10^{-4} mL mol g^{-2}) for HGS indicates net repulsive interactions and is consistent with the observation that HGS also does not undergo LLPS as noted above for BGS. The B_2 value for 2N-HGS is still positive but markedly smaller (7.1×10^{-4} mL mol g^{-2}), which is indicative of significantly weakened repulsive interactions following the deamidation of two Asn residues. Interestingly, the additional deamidation of two Gln residues in 2N-HGS to give 2N2Q-HGS changes the magnitude of B_2 much less (6.65×10^{-4} mL mol g^{-2}). Thus, the deamidation of Gln residues, whether due to their inherent chemistry or surface location, seems to have a smaller contribution in lowering B_2 further than that due to the deamidation of Asn residues alone.

To show the significance of the change in the sign and magnitude of B_2 to protein solubility and phase separation, we now draw from a variety of cases. Wilson[51] compiled the solution conditions for the crystallization of 50 different proteins and their corresponding B_2 values and found that the B_2 values ranged from −0.5 to −8.0×10^{-4} mL mol g^{-2}. Solution conditions that produced B_2 values lower than these (i.e., more negative) generally resulted

in amorphous precipitation of proteins, and when the B_2 values were more positive, they required a much higher concentration of proteins to show any phase separation. In another study, Guo et al.[52] found that for lysozyme in solution where its B_2 was almost 0 mL mol g^{-2}, has solubility of ~55 mg/mL, but when B_2 dropped to -2×10^{-4} mL mol g^{-2}, the solubility decreased by a factor of two. Similarly, for ovalbumin,[52] when B_2 is 0.2×10^{-4} mL mol g^{-2}, its solubility is 46.4 mg/mL but is reduced to one-third of this value when B_2 drops to -3.3×10^{-4} mL mol g^{-2}. A more familiar example is the effect of ammonium sulfate, a well-known generic protein precipitant, on the B_2 values of a protein. For equine serum albumin in 0.1 M acetate buffer (pH 5.6), B_2 values are 2.0, 1.1, 0.1, and -0.1×10^{-4} mL mol g^{-2} in the presence of 0, 0.5, 1.0, and 1.5 M ammonium sulfate, respectively,[53] suggesting an empirical correlation between the lowering of B_2 and salting out (or the lowering of protein solubility) of a protein. Clearly, the solubilities of proteins tend to drop as the net attraction between proteins increases and B_2 values become less positive.

Using PEG to induce LLPS as described by Annunziata et al.[45] with BGS and Wang et al.[37] with the immunoglobulins, we examined the phase behavior of HGS and its mutants. The data shown in Figure 6A (and inset) suggest that the fraction of deamidated protein derivatives (2N-HGS and 2N2Q-HGS) populating the condensed phase (i.e., precipitated or high-density phase) is larger than that of HGS. Thus, in our model system, for the same concentration of PEG, more of the deamidated derivatives were found in the condensed phase compared to the wild-type protein, again suggestive of an increased level of attraction among the deamidated derivatives relative to that of wild-type HGS. This is a clear illustration of the weakening of repulsive interaction upon deamidation. Analysis of this data (see Experimental Procedures, Figure 6B, and Table 1) provides E_B, the excess binding energy due to the deamidation in the condensed phase.[37] Its magnitude is rather small, ~1 kJ/mol, a value comparable to that of the weakest hydrogen bonds.[54] Note however that the binding energy in the condensed phase signifies the average interaction of the protein with its neighbors. Thus, the small change in binding energy following deamidation observed in our experiments could result from a strong but localized attraction between the deamidated protein molecule and its neighbors. It needs to be emphasized that PEG in our experiments is only a tool to induce liquid–liquid phase separation. This is known to occur due to excluded volume effects,[37] just as in PEG-induced protein crystallization.[55] PEG itself does not penetrate into the condensed phase and E_B, obtained by the analysis of the PEG-induced LLPS, is not dependent on, or related to PEG, but is an independent intrinsic property of the deamidated proteins in the condensed phase.

Our data clearly suggest that deamidation weakens the net repulsive self-interaction in HGS and is likely to diminish the "protective role" ascribed to GS.[46] While experiments similar to those of Liu et al.[46,47] may provide a quantitative measure of the effect of deamidation on the diminution of such a protective role, a larger question is the effect of deamidation *in vivo*, in the cellular environment of the lens. Within the fiber cell, where protein concentrations are known to approach those in protein crystals, macromolecular crowding is an important factor and excluded volume effects are likely to favor attractive protein–protein interaction.[56] In view of that fact, that PEG is also often used in solution to simulate macromolecular crowding *in vivo*,[57] we note that the same concentration of PEG partitions more of the deamidated proteins to the condensed phase compared to the native (Figure 6A).

Thus, our data suggest that deamidation would facilitate the condensation of HGS *in vivo* as well, a likely scenario also inferred from the reduction in B_2 (Figure 5 and Table 1). Clearly, that would also lower the effectiveness of HGS in protecting against the aggregation and condensation of the other γ-crystallins.[46,47]

We are aware that results from the PEG experiments performed *in vitro* cannot truly mimic molecular crowding *in vivo*, because of the inherent complexity and dynamics within the cell. In fact, in general, results obtained in solution *in vitro* cannot be expected to mimic the *in vivo* situation entirely. However, often the effects observed *in vivo* can be replicated *in vitro*. A vivid example is the work of Kmoch et al.,[58] who extracted crystals of the pure R36S mutant of HGD from the fiber cells of a juvenile cataract patient, even though it was an autosomal dominant mutation; the mutant protein *in vitro* also crystallizes spontaneously and shows a dramatic decrease in its solubility.[48] This is by no means an isolated case of a single protein *in vivo* behaving like it does *in vitro*. Another, equally dramatic example is the gelation of hemoglobin-S *in vitro*,[59] which mimics the gelation that occurs *in vivo*,[60] and much progress has been achieved in this area because so much could be learned about the gelation process *in vitro*.[61] For several cataract-associated γ-crystallins, we have observed that they also show attractive self-interactions in solution *in vitro*,[33,48,49] a clear indicator of susceptibility to protein condensation. Thus, it appears that when the attractive self-interactions are strong in a protein, they override other interactions, even within the crowded and diverse cellular environment, and protein condensation occurs.

However, we recognize that a γ-crystallin mutation characterized by unaltered self-interaction (compared to that of the wild type) may be involved in interactions with other crystallins to produce deleterious changes. We showed this for the cataract-associated E107A mutant of HGD, which exhibited a stronger (heterologous) interaction with a-crystallin and produced the density fluctuations that led to light scattering.[62] The work presented here is merely the first, direct evidence that even a limited deamidation (only four residues) leads to enhanced attractive self-interactions in a key lens protein, γS-crystallin, and has implications for lens opacity.

SUMMARY AND CONCLUSIONS

In this report, we have shown that deamidation of Asn residues 76 and 143 in human γS-crystallin results in weakening of the overall repulsive protein–protein interactions, thus rendering the deamidated product more prone to aggregation. This process would also compromise the beneficial effects exhibited by the protein in protecting the other γ-crystallins in the lens. The data suggest that the effect of additional deamidation of Gln92 and Gln120 is much weaker in enhancing the attractive interactions beyond that observed due to the deamidation of Asn residues alone. Upon deamidation, the secondary structures of the proteins remain intact, but minor changes are apparent in the tertiary structure, which do not appreciably alter the stability of the proteins. The pI of the proteins is lowered upon deamidation, as expected, but does not produce a significant change in either protein structure or stability. We recognize that the observed effects of deamidation *in vivo* may result from other, subsequent changes at the deamidated sites, such as racemization and isomerization,[16,26] but a recent report did not find evidence that any Asp residue in γS-

crystallin or other γ-crystallins was either racemized or isomerized.[63] This is clearly an important observation that contradicts earlier reports[26] and merits further investigation in the department of biology at the University at Albany.

Supplementary Material

Refer to Web version on PubMed Central for supplementary material.

Acknowledgments

ABBREVIATIONS

BGS	bovine γS-crystallin
B_2	second virial coefficient
CD	circular dichroism
ESIMS	electrospray ionization mass spectrometry
GdnHCl	guanidinium hydrochloride
GS	γS-crystallin
HGS	human γS-crystallin
IEF	isoelectric focusing
pI	isoelectric point
IPTG	isopropyl β-D-1-thiogalactopyrano-side
LLPS	liquid–liquid phase separation
PEG	polyethylene glycol
PTMs	post-translational modifications
SDS–PAGE	sodium dodecyl sulfate–polyacrylamide gel electrophoresis
UV	ultraviolet

References

1. Dasari S, Wilmarth PA, Rustvold DL, Riviere MA, Nagalla SR, David LL. Reliable detection of deamidated peptides from lens Crystallin proteins using changes in reversed-phase elution times and parent ion masses. J Proteome Res. 2007; 6:3819–3826. [PubMed: 17696381]

2. Robinson NE, Robinson AB. Deamidation of human proteins. Proc Natl Acad Sci U S A. 2001; 98:12409–12413. [PubMed: 11606750]

3. Takemoto L, Fujii N, Boyle D. Mechanism of asparagine deamidation during human senile cataractogenesis. Exp Eye Res. 2001; 72:559–563. [PubMed: 11311047]

4. Araki N, Moini M. Age estimation of museum wool textiles from Ovis aries using deamidation rates utilizing matrix-assisted laser desorption/ionization time-of-flight mass spectrometry. Rapid Commun Mass Spectrom. 2011; 25:3396–3400. [PubMed: 22002692]

5. Leo G, Bonaduce I, Andreotti A, Marino G, Pucci P, Colombini MP, Birolo L. Deamidation at asparagine and glutamine as a major modification upon deterioration/aging of proteinaceous binders in mural paintings. Anal Chem. 2011; 83:2056–2064. [PubMed: 21348436]

6. Riha WE 3rd, Izzo HV, Zhang J, Ho CT. Nonenzymatic deamidation of food proteins. Crit Rev Food Sci Nutr. 1996; 36:225–255. [PubMed: 8744605]

7. Robinson NE, Robinson AB. Prediction of protein deamidation rates from primary and three-dimensional structure. Proc Natl Acad Sci U S A. 2001; 98:4367–4372. [PubMed: 11296285]

8. Xie M, Schowen RL. Secondary structure and protein deamidation. J Pharm Sci. 1999; 88:8–13. [PubMed: 9874696]

9. Kosky AA, Razzaq UO, Treuheit MJ, Brems DN. The effects of alpha-helix on the stability of Asn residues: deamidation rates in peptides of varying helicity. Protein science: a publication of the Protein Society. 1999; 8:2519–2523. [PubMed: 10595558]

10. Kossiakoff AA. Tertiary structure is a principal determinant to protein deamidation. Science. 1988; 240:191–194. [PubMed: 3353715]

11. Lapko VN, Purkiss AG, Smith DL, Smith JB. Deamidation in human gamma S-Crystallin from cataractous lenses is influenced by surface exposure. Biochemistry. 2002; 41:8638–8648. [PubMed: 12093281]

12. Stratton LP, Kelly RM, Rowe J, Shively JE, Smith DD, Carpenter JF, Manning MC. Controlling deamidation rates in a model peptide: effects of temperature, peptide concentration, and additives. J Pharm Sci. 2001; 90:2141–2148. [PubMed: 11745773]

13. Hao P, Ren Y, Alpert AJ, Sze SK. Detection, evaluation and minimization of nonenzymatic deamidation in proteomic sample preparation. Mol Cell Proteomics. 2011; 10:O111.009381.

14. Yuan PM, Talent JM, Gracy RW. Molecular basis for the accumulation of acidic isozymes of triosephosphate isomerase on aging. Mech Ageing Dev. 1981; 17:151–162. [PubMed: 7311622]

15. Cini JK, Gracy RW. Molecular basis of the isozymes of bovine glucose-6-phosphate isomerase. Arch Biochem Biophys. 1986; 249:500–505. [PubMed: 3753014]

16. Lampi KJ, Wilmarth PA, Murray MR, David LL. Lens beta-crystallins: the role of deamidation and related modifications in aging and cataract. Prog Biophys Mol Biol. 2014; 115:21–31. [PubMed: 24613629]

17. Dilley KJ, Harding JJ. Changes in proteins of the human lens in development and aging. Biochim Biophys Acta, Protein Struct. 1975; 386:391–408.

18. Van Kleef SM, Willems-Thijssen W, Hoenders HJ. Intracellular degradation and deamidation of alpha-Crystallin subunits. Eur J Biochem. 1976; 66:477–483. [PubMed: 954752]

19. Chaves JM, Srivastava K, Gupta R, Srivastava OP. Structural and functional roles of deamidation and/or truncation of N- or C-termini in human alpha A-Crystallin. Biochemistry. 2008; 47:10069–10083. [PubMed: 18754677]

20. Gupta R, Srivastava OP. Effect of deamidation of asparagine 146 on functional and structural properties of human lens alphaB-Crystallin. Invest Ophthalmol Visual Sci. 2004; 45:206–214. [PubMed: 14691175]

21. Takata T, Oxford JT, Demeler B, Lampi KJ. Deamidation destabilizes and triggers aggregation of a lens protein, betaA3-Crystallin. Protein Sci. 2008; 17:1565–1575. [PubMed: 18567786]

22. Lampi KJ, Amyx KK, Ahmann P, Steel EA. Deamidation in human lens betaB2-Crystallin destabilizes the dimer. Biochemistry. 2006; 45:3146–3153. [PubMed: 16519509]

23. Flaugh SL, Mills IA, King J. Glutamine deamidation destabilizes human gammaD-Crystallin and lowers the kinetic barrier to unfolding. J Biol Chem. 2006; 281:30782–30793. [PubMed: 16891314]

24. Hooi MY, Raftery MJ, Truscott RJ. Age-dependent deamidation of glutamine residues in human gammaS Crystallin: deamidation and unstructured regions. Protein science: a publication of the Protein Society. 2012; 21:1074–1079. [PubMed: 22593035]

25. Takemoto L, Boyle D. Increased deamidation of asparagine during human senile cataractogenesis. Molecular vision. 2000; 6:164–168. [PubMed: 10976112]

26. Hooi MY, Raftery MJ, Truscott RJ. Racemization of two proteins over our lifespan: deamidation of asparagine 76 in gammaS Crystallin is greater in cataract than in normal lenses across the age range. Invest Ophthalmol Visual Sci. 2012; 53:3554–3561. [PubMed: 22531704]

27. Takemoto L. Deamidation of Asn-143 of gammaS Crystallin from protein aggregates of the human lens. Curr Eye Res. 2001; 22:148–153. [PubMed: 11402392]

28. Tsur D, Tanner S, Zandi E, Bafna V, Pevzner PA. Identification of post-translational modifications by blind search of mass spectra. Nat Biotechnol. 2005; 23:1562–1567. [PubMed: 16311586]

29. Wilmarth PA, Tanner S, Dasari S, Nagalla SR, Riviere MA, Bafna V, Pevzner PA, David LL. Age-related changes in human crystallins determined from comparative analysis of post-translational modifications in young and aged lens: does deamidation contribute to Crystallin insolubility? J Proteome Res. 2006; 5:2554–2566. [PubMed: 17022627]

30. Hanson SR, Smith DL, Smith JB. Deamidation and disulfide bonding in human lens gamma-crystallins. Exp Eye Res. 1998; 67:301–312. [PubMed: 9778411]

31. Hains PG, Truscott RJ. Age-dependent deamidation of lifelong proteins in the human lens. Invest Ophthalmol Visual Sci. 2010; 51:3107–3114. [PubMed: 20053973]

32. Takata T, Oxford JT, Brandon TR, Lampi KJ. Deamidation alters the structure and decreases the stability of human lens betaA3-Crystallin. Biochemistry. 2007; 46:8861–8871. [PubMed: 17616172]

33. Pande A, Pande J, Asherie N, Lomakin A, Ogun O, King JA, Lubsen NH, Walton D, Benedek GB. Molecular basis of a progressive juvenile-onset hereditary cataract. Proc Natl Acad Sci U S A. 2000; 97:1993–1998. [PubMed: 10688888]

34. Zhao H, Brown PH, Schuck P. On the distribution of protein refractive index increments. Biophys J. 2011; 100:2309–2317. [PubMed: 21539801]

35. Zhao H, Brown PH, Magone MT, Schuck P. The molecular refractive function of lens gamma-Crystallins. J Mol Biol. 2011; 411:680–699. [PubMed: 21684289]

36. Yadav S, Scherer TM, Shire SJ, Kalonia DS. Use of dynamic light scattering to determine second virial coefficient in a semidilute concentration regime. Anal Biochem. 2011; 411:292–296. [PubMed: 21156151]

37. Wang Y, Latypov RF, Lomakin A, Meyer JA, Kerwin BA, Vunnum S, Benedek GB. Quantitative evaluation of colloidal stability of antibody solutions using PEG-induced liquid-liquid phase separation. Mol Pharmaceutics. 2014; 11:1391–1402.

38. Kelly SM, Jess TJ, Price NC. How to study proteins by circular dichroism. Biochim Biophys Acta, Proteins Proteomics. 2005; 1751:119–139.

39. Zarina S, Slingsby C, Jaenicke R, Zaidi ZH, Driessen H, Srinivasan N. Three-dimensional model and quaternary structure of the human eye lens protein gamma S-Crystallin based on beta- and gamma-Crystallin X-ray coordinates and ultracentrifugation. Protein Sci. 1994; 3:1840–1846. [PubMed: 7849599]

40. Pace CN. Determination and analysis of urea and guanidine hydrochloride denaturation curves. Methods Enzymol. 1986; 131:266–280. [PubMed: 3773761]

41. Kingsley CN, Brubaker WD, Markovic S, Diehl A, Brindley AJ, Oschkinat H, Martin RW. Preferential and specific binding of human alphaB-Crystallin to a cataract-related variant of gammaS-Crystallin. Structure. 2013; 21:2221–2227. [PubMed: 24183572]

42. Kim YH, Kapfer DM, Boekhorst J, Lubsen NH, Bachinger HP, Shearer TR, David LL, Feix JB, Lampi KJ. Deamidation, but not truncation, decreases the urea stability of a lens structural protein, betaB1-Crystallin. Biochemistry. 2002; 41:14076–14084. [PubMed: 12437365]

43. van Dam AF. Purification and composition of beta-s-Crystallin. Exp Eye Res. 1966; 5:255–266. [PubMed: 5954516]

44. Quax-Jeuken Y, Driessen H, Leunissen J, Quax W, de Jong W, Bloemendal H. beta s-Crystallin: structure and evolution of a distinct member of the beta gamma-superfamily. EMBO J. 1985; 4:2597–2602. [PubMed: 4054100]

45. Annunziata O, Ogun O, Benedek GB. Observation of liquid-liquid phase separation for eye lens gammaS-Crystallin. Proc Natl Acad Sci U S A. 2003; 100:970–974. [PubMed: 12529503]

46. Liu C, Asherie N, Lomakin A, Pande J, Ogun O, Benedek GB. Phase separation in aqueous solutions of lens gamma-crystallins: special role of gamma s. Proc Natl Acad Sci U S A. 1996; 93:377–382. [PubMed: 8552642]

47. Liu C, Pande J, Lomakin A, Ogun O, Benedek GB. Aggregation in aqueous solutions of bovine lens gamma-crystallins: special role of gamma(s). Invest Ophthalmol Visual Sci. 1998; 39:1609–1619. [PubMed: 9699550]

48. Pande A, Pande J, Asherie N, Lomakin A, Ogun O, King J, Benedek GB. Crystal cataracts: human genetic cataract caused by protein crystallization. Proc Natl Acad Sci U S A. 2001; 98:6116–6120. [PubMed: 11371638]

49. Pande A, Annunziata O, Asherie N, Ogun O, Benedek GB, Pande J. Decrease in protein solubility and cataract formation caused by the Pro23 to Thr mutation in human gamma D-Crystallin. Biochemistry. 2005; 44:2491–2500. [PubMed: 15709761]

50. Tardieu A, Veretout F, Krop B, Slingsby C. Protein interactions in the calf eye lens: interactions between beta-crystallins are repulsive whereas in gamma-crystallins they are attractive. Eur Biophys J. 1992; 21:1–12. [PubMed: 1516556]

51. Wilson WW. Light scattering as a diagnostic for protein crystal growth–a practical approach. J Struct Biol. 2003; 142:56–65. [PubMed: 12718919]

52. Guo B, Kao S, McDonald H, Asanov A, Combs LL, Wilson WW. Correlation of second virial coefficients and solubilities useful in protein crystal growth. J Cryst Growth. 1999; 196:424–433.

53. Demoruelle K, Guo B, Kao S, McDonald HM, Nikic DB, Holman SC, Wilson WW. Correlation between the osmotic second virial coefficient and solubility for equine serum albumin and ovalbumin. Acta Crystallogr, Sect D: Biol Crystallogr. 2002; 58:1544–1548. [PubMed: 12351858]

54. Gilli, G., Gilli, P. The nature of the hydrogen bond: Outline of a comprehensive hydrogen bond theory. Oxford University Press; Oxford, U.K: 2009.

55. Piazza R. Interactions and phase transitions in protein solutions. Curr Opin Colloid Interface Sci. 2000; 5:38–43.

56. Annunziata O, Asherie N, Lomakin A, Pande J, Ogun O, Benedek GB. Effect of polyethylene glycol on the liquid-liquid phase transition in aqueous protein solutions. Proc Natl Acad Sci U S A. 2002; 99:14165–14170. [PubMed: 12391331]

57. Boersma AJ, Zuhorn IS, Poolman B. A sensor for quantification of macromolecular crowding in living cells. Nat Methods. 2015; 12:227–229. [PubMed: 25643150]

58. Kmoch S, Brynda J, Asfaw B, Bezouska K, Novak P, Rezacova P, Ondrova L, Filipec M, Sedlacek J, Elleder M. Link between a novel human gammaD-Crystallin allele and a unique cataract phenotype explained by protein crystallography. Hum Mol Genet. 2000; 9:1779–1786. [PubMed: 10915766]

59. Eaton WA, Hofrichter J. Sickle cell hemoglobin polymerization. Adv Protein Chem. 1990; 40:63–279. [PubMed: 2195851]

60. Coletta M, Hofrichter J, Ferrone FA, Eaton WA. Kinetics of sickle haemoglobin polymerization in single red cells. Nature. 1982; 300:194–197. [PubMed: 7133139]

61. Ferrone FA. The delay time in sickle cell disease after 40 years: A paradigm assessed. Am J Hematol. 2015; 90:438–445. [PubMed: 25645011]

62. Banerjee PR, Pande A, Patrosz J, Thurston GM, Pande J. Cataract-associated mutant E107A of human gammaD-Crystallin shows increased attraction to alpha-Crystallin and enhanced light scattering. Proc Natl Acad Sci U S A. 2011; 108:574–579. [PubMed: 21173272]

63. Sakaue H, Takata T, Fujii N, Sasaki H, Fujii N. Alpha B- and betaA3-crystallins containing d-aspartic acids exist in a monomeric state. Biochim Biophys Acta, Proteins Proteomics. 2015; 1854:1–9.
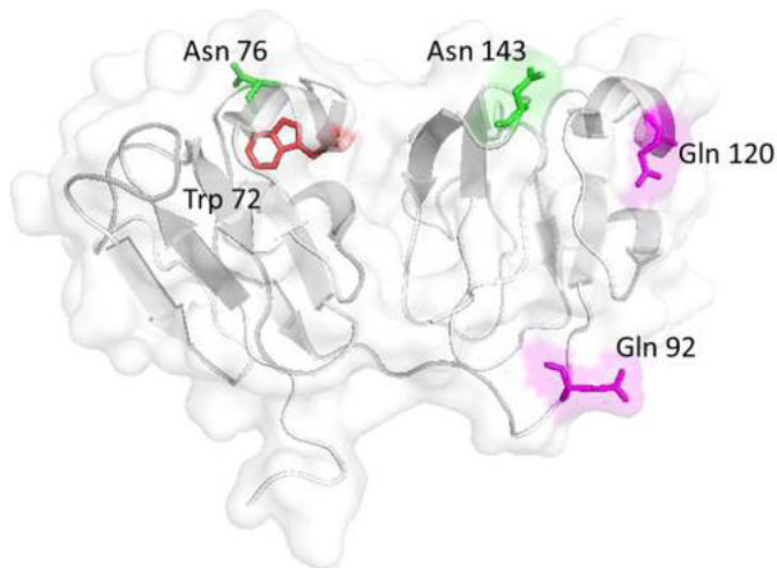
Figure 1.
Surface representation of HGS based on its NMR structure[41] (Protein Data Bank entry 2M3T) (gray) showing the four modified residues, Asn76 and Asn143 (green), and Gln92 and Gln120 (magenta). Gln120 is part of the small helical segment, while the other three are in the unstructured regions of the protein. Trp72, the only Trp residue close to any of the modified residues, is located ~3 Å from Asn76. The residue numbering corresponds to the actual numbers in the protein, which represents one fewer residue than that used in the NMR data with an additional Gly at position 1. Figure drawn using Pymol.
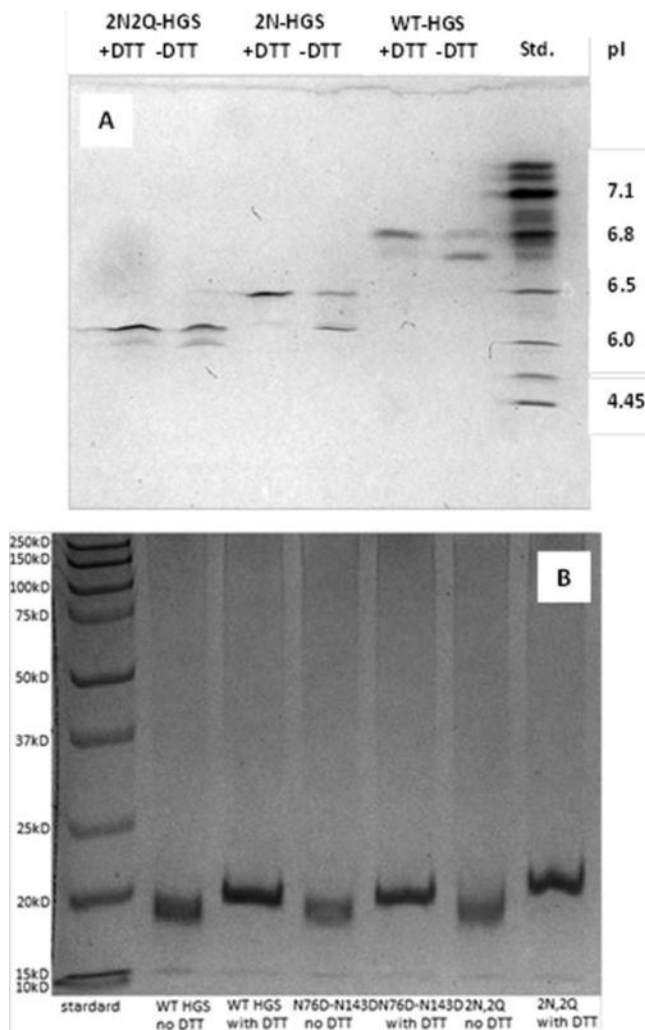
Figure 2.
IEF and SDS–PAGE analysis of HGS and the two deamidated proteins with and without DTT. (A) Representative IEF gel showing pI values of 6.9, 6.5, and 6.1 for HGS, 2N-HGS, and 2N2Q-HGS, respectively (average of three runs). The two bands merge into a single component following DTT treatment. (B) SDS–PAGE analysis showing that all three proteins are monomeric with a molecular mass of ~20 kDa. The molecular masses are slightly but consistently higher after reduction with DTT.
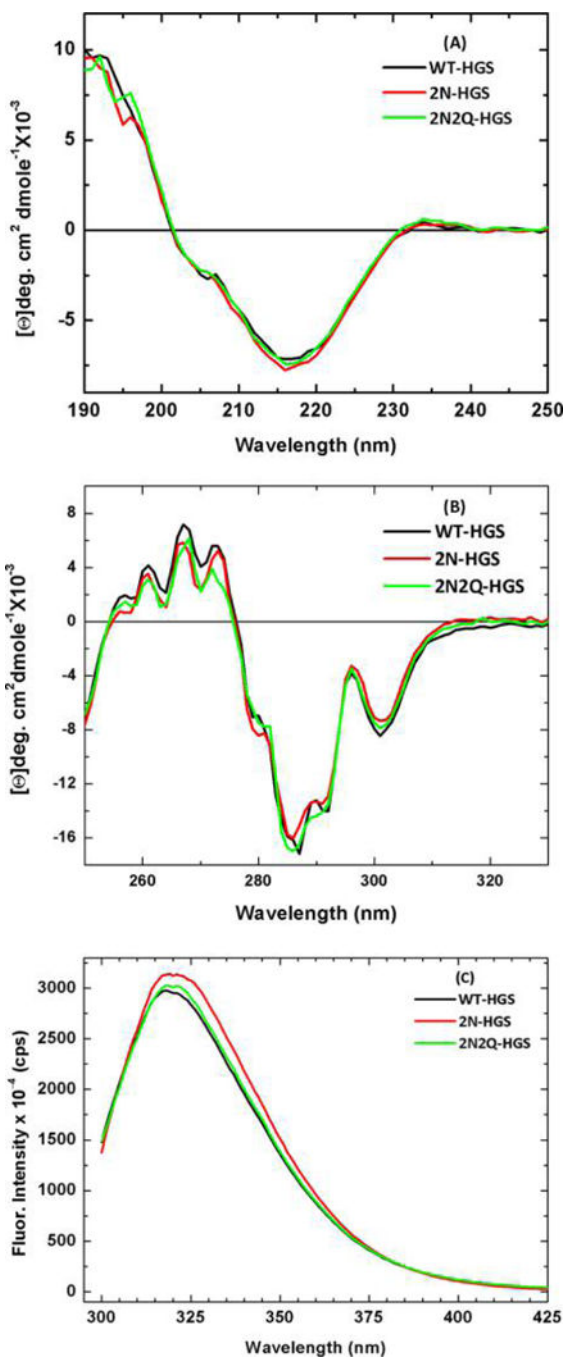
Figure 3.
(A) Far-UV, (B) near-UV, and (C) tryptophan fluorescence emission spectra of HGS, 2N-HGS, and 2N2Q-HGS. Protein concentrations of 0.1 mg/mL (far-UV CD and fluorescence) and 1.0 mg/mL (near-UV CD). Path lengths of 1 mm (far-UV CD) and 10 mm (near-UV CD and fluorescence). Spectra were measured in 0.1 M sodium phosphate buffer (pH 7).
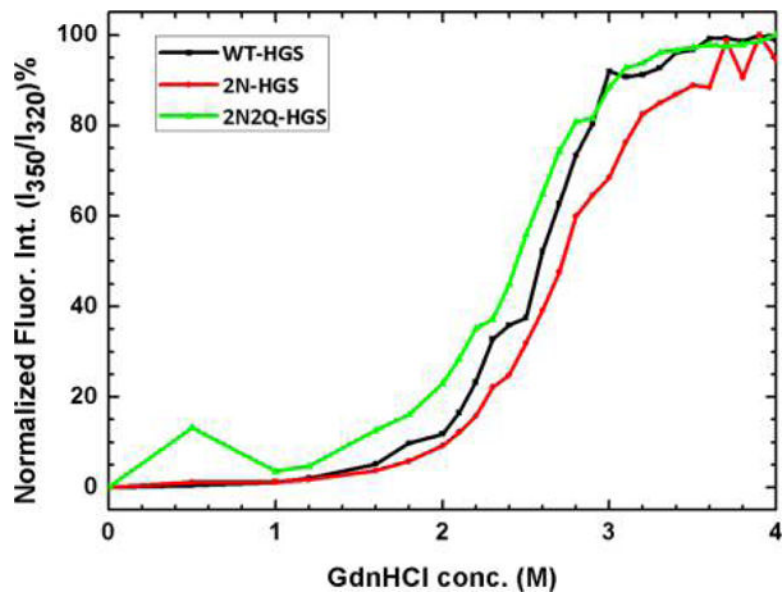
Figure 4.
Comparison of the chemical stabilities of HGS, 2N-HGS, and 2N2Q-HGS as a function of GdnHCl concentration. All three proteins show comparable stabilities with a transition midpoint of 2.6 ± 0.1 M GdnHCl. Protein concentration of 0.1 mg/mL in 0.1 M sodium phosphate (pH 7). The lines drawn through the data are visual guides.
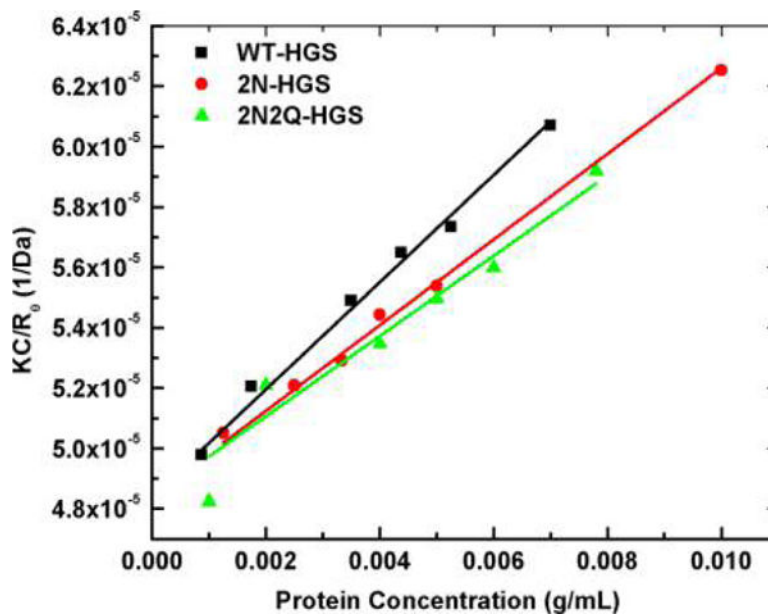
Figure 5.
Debye plots calculated from static light scattering data taken with a Zetasizer Nano-S (Malvern Instruments). Protein samples were measured in 0.1 M sodium phosphate buffer (pH 7) at 25 °C. Global fitting of the three data sets, keeping the intercept identical, was performed using Origin 9.1 (Origin Lab). The molecular weights obtained from the *Y*-axis intercept (eq 1) are in agreement with those calculated from the protein sequence.
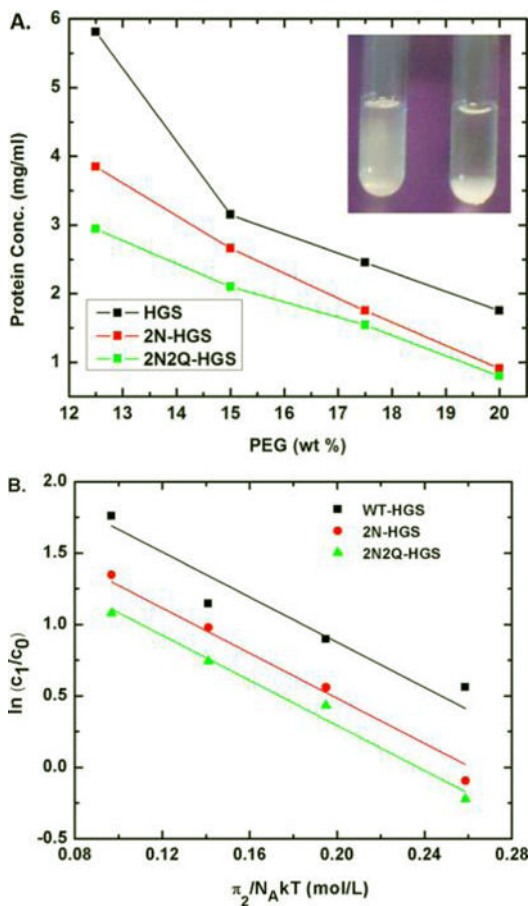
Figure 6.
(A) Plot of the equilibrium concentrations of HGS and its deamidated derivatives 2N-HGS and 2N2Q-HGS in the supernatant after incubation at 4 °C, as a function of the initial PEG (8000K) concentration. The initial concentration of all proteins was 6.25 mg/ mL. Each datum point is an average of three replicates. The lines drawn through the data are visual guides. The inset shows a photograph of PEG-induced phase separation resulting in cloudy protein solutions (left), and the dense and dilute phases are clearly distinguishable at equilibrium after 24 h at 4 °C (right). (B) Analysis of the data shown in panel A, using eq 2. The intercept of the plots provides E_B, the binding energy of the protein in the condensed phase.[37] E_B values are calculated from the lowering of chemical potential in the condensed phase of the mutant relative to that in HGS.

Table 1

Comparison of B_2 Values (second virial coefficient), Molecular Weights, and Excess Binding Energies for HGS and the Deamidated Mutants[a]

protein	B_2 (mL mol g^{-2}) (second virial coefficient)	estimated molecular weight (kDa) from the Debye plot[b]	known molecular weight (expasy.ch)	E_B[c] (kJ/mol) (excess binding energy in the condensed phase)
HGS	$8.90 \times 10^{-4} \pm 7.8 \times 10^{-5}$	20.66 ± 0.10	20876	0
2N-HGS	$7.10 \times 10^{-4} \pm 6.4 \times 10^{-5}$	20.66 ± 0.10	20878	0.9 ± 0.4
2N2Q-HGS	$6.65 \times 10^{-4} \pm 6.9 \times 10^{-5}$	20.66 ± 0.30	20880	1.4 ± 0.6

[a]B_2 values were calculated from the Debye plot shown in Figure 5.

[b]From global fitting of the data constrained to the same intercept in Figure 6B.

[c] E_B was obtained from the plots in Figure 6A,B, as described by Wang et al.,[37] and calculated from the lowering of the chemical potential in the condensed phase *relative* to HGS. Note that E_B here is equivalent to $N_A e_B$ in ref 37.